Supporting Information

Multilobular morphology: the key for biphase multifunctional nanogels

A.S. Sonzogni[1], S. Hamzehlou[2], V. D.G. Gonzalez[1], J. R. Leiza[2], R. J. Minari[1]

1. Group of Polymers and Polymerization Reactors, INTEC (Universidad Nacional del Litoral-CONICET), Güemes 3450, Santa Fe 3000, Argentina
2. POLYMAT, Kimika Aplikatua saila, Kimika Zientzien Fakultatea, University of the Basque Country UPV/EHU, Joxe Mari Korta Zentroa, Tolosa Hiribidea 72, 20018, Donostia/San Sebastián, Spain

Synthesis of mLNGS

The same recipe was used for the synthesis of mLNGs-1 and mLNGs-2 as displayed in **Table S1**. Dosing VCL emulsion also incorporates $NaHCO_3$ as buffer in order to avoid VCL hydrolysis, which can occur because the acidification of the media for the presence of KPS.[1]

Table S1. Detailed recipe of semibatch synthesis of mLNG.

Reagent mass	**Initial load [%wbvcl*]**	**VCL emulsion [%wbvcl*]**	**BA emulsion [%wbvcl*]**
VCL	50	50	0
BA	0	0	66
BIS	4	0	0
KPS			
SDS	2	2	0.33
$NaHCO_3$	0.5	0.5	-
Water	770	770	133

*wbvcl = Weight based on VCL

Monomers conversion was determined by ^{1}H NMR by following the vinyl bond signal of each monomer (region around 7 ppm for VCL and 6 ppm for BA). **Figure S1** shows the NMR spectra of a sample taken 10 min after the beginning of BA dosification (t_i^{dos}) in mLNGs-1 and mLNGs-2 and at the end of both polymerizations.

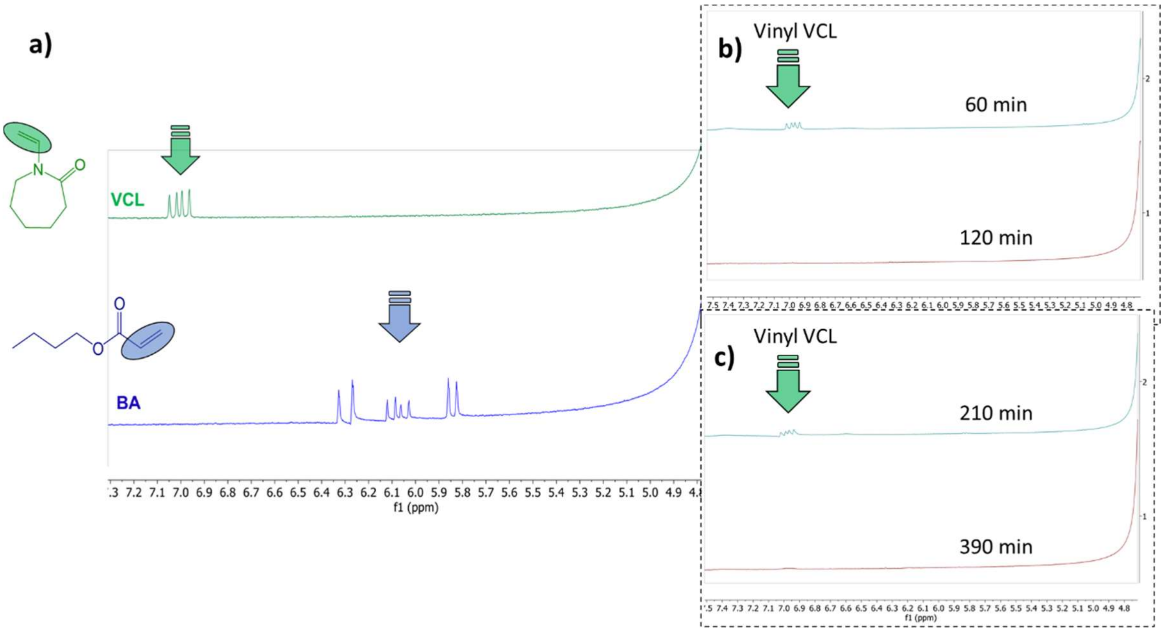

Figure S1. Zoom of ^{1}H NMR spectra in the vinyl region for pure VCL and BA monomers (**a**) and for samples taken 10 min after beginning BA dosification and at the end of polymerization in mLNGs-1 (**b**) and mLNGs-2 (**c**).

Figure S2 shows the dDSC thermograms for both mLNGs synthesized samples. Both thermograms present two phases with different Tg values. The peak at high temperature corresponds to the glass transition of crosslinked PVCL phase which presents a maximum at around 195°C. This Tg value is close to that reported by Imaz et al.[2] for the PVCL NGs with BIS as crosslinker (200°C), which resulted higher than the Tg value of the linear PVCL (147 °C)[3] because it was densely crosslinked. An additional peak is observed at lower temperatures in both samples. In mLNG-1, it is observed a very wide glass transition in the range temperature from -40 to 40°C, with a maximum around 0°C, and in mLNGs-2 a narrower Tg with a maximum around -20°C.

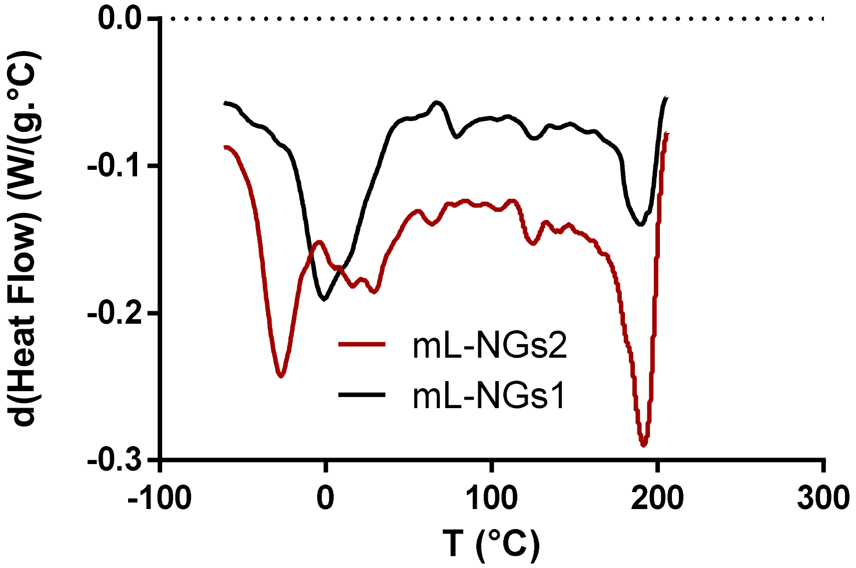

Figure S2. dDSC thermograms of second heat of mLNGs-1 and mLNGs-2

Mathematical model

The model includes the material balances for the monomers and polymer formed during the second stage of polymerization ($pol2$) and the population balances for the clusters (see reference [4] and [5] for details). Herein an illustration of the equilibrium and non-equilibrium positions considered in the model, the population balances of clusters as well as equations to solve radical concentration profile are presented.

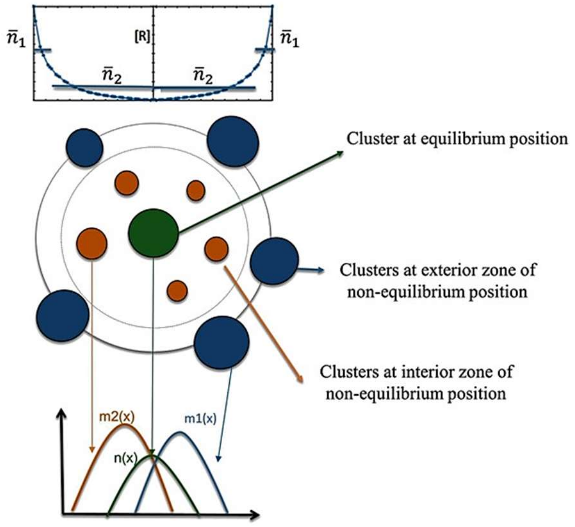

Figure S3. Illustration of the equilibrium and non-equilibrium positions considered in the mathematical model. Reprinted from reference [4].

The population balances for the clusters of size x (number of polymerized monomer units) at non-equilibrium positions (m1 and m2) and clusters at equilibrium position (n) are as follows:

Population balance for clusters at exterior non-equilibrium positions:

$$\frac{\mathrm{dm1(x)}}{\mathrm{dt}} = \left(1-\delta_{x_c}\right) r_p^{m1}(x-1)\,m1(x-1) - r_p^{m1}(x)\,m1(x)$$

Propagation

$$+\left(1-\delta_{xc}\right) r_d^{m1}(x-\bar{x}_m)\, m1(x-\bar{x}_m) - r_d^{m1}(x)\,m1(x)$$

Polymer diffusion from polymer matrix

$$+\left(1-\delta_{x\le 2x_c}\right)\alpha_m(x)\frac{k_a}{V_p}\left(1-\frac{1}{m1_{av}}\right)\int_{x_c}^{x-x_c} m1(z)\,m1(x-z)\,dz$$

$$-2m1(x)\frac{k_a}{V_p}\left(1-\frac{1}{m1_{av}}\right)\int_{x_c}^{x_{max}-x} \alpha_m(x+z)\,m1(z)\,dz$$

Cluster coalescence

$$-k_{mov1}\,m1(x)$$

Movement to interior non-equilibrium region

$$+k_{mov3}m2(x)$$

Backward movement to exterior non-equilibrium region

$$+\delta_{x_c}r_{nuc}$$

Cluster nucleation (S1)

The first line in the right hand side of equation S1 refers to cluster growth by polymerization with a rate of r_p^{m1} (rate coefficient of $\bar{k}_p$) and the second line corresponds to the growth of the clusters by diffusion of Polymer 2 from the polymer matrix which occurs at the rate of r_d^{m1} (mass transfer rate coefficient of k_d^{pol2}). The next two integral terms accounts for cluster coagulation with rate coefficient of k_a. Clusters movement to interior non-equilibrium region and backward movement to exterior non-equilibium region due to cluster-water van der Waals forces with rate coefficients of k_{mov1} and k_{mov3} are accounted in the model. The last term in equation S1 refers to cluster nucleation at the rate of r_{nuc} (with rate coefficient of k_n). Note that δ is equal to one if the condition in its subscript is fulfilled.

Rates of $r_p^{m1}(x)$, $r_d^{m1}(x)$ and r_{nuc} are given by:

$$r_p^{m1}(x) = \bar{k}_p \frac{\bar{n}_1 N_p}{N_a} \frac{M}{V_1} \phi_x \tag{S2}$$

$$\phi_x = \frac{x}{(pol1 + pol2)N_A} \tag{S3}$$

$$r_d^{m1}(x) = \frac{k_d^{pol2} \phi a_{m1}(x) N_A}{\bar{x}_m} \tag{S4}$$

$$r_{nuc} = \frac{k_n \phi N_A}{x_c} \tag{S5}$$

where $\bar{x}_m$ being the kinetic chain length of Polymer 2, V_1 is the volume of region 1, a_{m1} is the surface area of the clusters in region 1, x_c is the size of the newly nucleated cluster that within a certain range, this size does not affect the particle morphology.[5] ϕ is excess of Polymer 2 in the polymer matrix with respect to the equilibrium condition given by:

$$\phi = \phi_2^H - \phi_2^c = \left\{ \begin{matrix} \phi_2^H - \phi_2^c & if\, \phi_2^H > \phi_2^c \\ 0 & otherwise \end{matrix} \right\} \qquad (S6)$$

where ϕ_2^H is the actual volume fraction of Polymer 2 in the matrix and ϕ_2^c is the volume fraction of the Polymer 2 in the matrix under equilibrium conditions.

The coefficients were defined in the model with following expressions:

$$k_{mov1} = \frac{k_{mov1\_0}}{{\phi_P}^5 * A * exp\left(\frac{B}{\left(\frac{T}{T_{g_{effective,matrix}}} - 0.866\right)}\right)} * \frac{V_{pol1,region1}}{V_{pol2,region1} + V_{pol1,region1}} \qquad (S7)$$

$$k_{mov2} = \frac{k_{mov2\_0}}{{\phi_P}^5 * A * exp\left(\frac{B}{\left(\frac{T}{T_{g_{effective,matrix}}} - 0.866\right)}\right)} \qquad (S8)$$

$$k_{mov3} = \frac{k_{mov3\_0}}{{\phi_P}^5 * A * exp\left(\frac{B}{\left(\frac{T}{T_{g_{effective,matrix}}} - 0.866\right)}\right)} * \frac{V_{pol2,region1}}{V_{pol2,region1} + V_{pol1,regi}} \qquad (S9)$$

$$k_d^{pol2} = \frac{k_{d0}^{pol2}}{{\phi_P}^5 * A * exp\left(\frac{B}{\left(\frac{T}{Tg_{effective,matrix}} - 0.866\right)}\right)} \qquad (S10)$$

where A, B, k_{mov1_0} , k_{mov2_0}, k_{mov3_0} and k_{d0}^{pol2} are adjustable parameters of the model. $V_{pol2,region1}$ is the volume of the second phase polymer in the exterior region of the particle (region 1), $V_{pol\ ,region1}$ is the volume of the seed in region 1 and $\mathrm{Tg}_{\mathrm{effective}}$ of the matrix is calculated as:

$$\mathrm{Tg}_{effective,matrix} = \frac{Tg_p + (\kappa Tg_M - Tg_P)\emptyset_M}{1 + (\kappa - 1)\phi_M} \qquad (S11)$$

where Tg_{p} is considered as the Tg of polymer from seed and κ is 1. A coalescence coefficients (k_a) was calculated as follow:

$$k_a = \frac{k_{a0}}{{\phi_P}^5 * \mathrm{A} * \exp\left(\frac{B}{\left(\frac{T}{Tg_{effective,\,2^{nd}polymer}} - 0.866\right)}\right)} \qquad (S12)$$

where, k_{a0} is adjustable parameter of the model.

The population balances for clusters at interior non-equilibrium position and for clusters at equilibrium positons are given in equations S13 and S14, respectively.

<u>Population balance for clusters at interior non-equilibrium position:</u>

$$\frac{\mathrm{dm2(x)}}{\mathrm{dt}} = \left(1 - \delta_{x_c}\right)\mathrm{r}_\mathrm{p}^{\mathrm{m2}}(\mathrm{x}-1)\mathrm{m2}(\mathrm{x}-1) - \mathrm{r}_\mathrm{p}^{\mathrm{m2}}(\mathrm{x})\mathrm{m2}(\mathrm{x})$$

<u>Propagation</u>

$$+ (1 - \delta_{\mathrm{xc}})\mathrm{r}_\mathrm{d}^{\mathrm{m2}}(\mathrm{x} - \bar{\mathrm{x}}_\mathrm{m})\, \mathrm{m2}(\mathrm{x} - \bar{\mathrm{x}}_\mathrm{m}) - \mathrm{r}_\mathrm{d}^{\mathrm{m2}}(\mathrm{x})\mathrm{m2}(\mathrm{x})$$

Polymer diffusion from polymer matrix

$$+\left(1-\delta_{x\le 2x_c}\right)\alpha_m(x)\frac{k_a}{V_p}\left(1-\frac{1}{m2_{av}}\right)\int_{x_c}^{x-x_c} m2(z)m2(x-z)dz$$

$$-2m2(x)\frac{k_a}{V_p}\left(1-\frac{1}{m2_{av}}\right)\int_{x_c}^{x_{max}-x} \alpha_m(x+z)m2(z)\,dz$$

Cluster coalescence

$$+k_{mov1}m1(x)$$

Movement to interior non-equilibrium position

$$-k_{mov3}m2(x)$$

Backward movement to exterior non-equilibrium region

$$-m2(x)\frac{k_{mov2}}{V_p}\int_{x_c}^{x_{max}-x} \alpha_m(x+z)n(z)\,dz$$

Movement to equilibrium position

$+\ \delta_{x_c}r_{nuc}$ Cluster nucleation (S13)

Population balance for cluster at equilibrium position

$$\frac{dn(x)}{dt} = (1-\delta_{x_c})r_p^n(x-1)n(x-1) - r_p^n(x)n(x)$$

Propagation

$$+\ (1-\delta_{x_c})r_d^n(x-\bar{x}_m)\ n(x-\bar{x}_m) - r_d^n(x)n(x)$$

Polymer diffusion from polymer matrix

$$+\left(1-\delta_{x\le 2x_c}\right)\alpha_n(x)\frac{k_{mov2}}{V_p}\int_{x_c}^{x-x_c} m2(z)n(x-z)\,dz$$

$$-\ n(x)\frac{k_{mov2}}{V_p}\int_{x_c}^{x_{max}-x} \alpha_n(x+z)m2(z)dz$$

Movement to equilibrium position (S14)

Table S1. Values of parameters used in the mathematical model

Parameter	Value	Reference
A	1.36×10^{-5}	4
B	3.2	4
$\mathbf{k_{p,BA}}$ **(L/mol.s)**	$2.21 \times 10^{7} \exp(-17.9/\mathrm{RT})$	6
$\mathbf{k_{p,VCL}}$ **(L/mol.s)**	$1340@\ 70°\mathrm{C}$	7
$\mathbf{r_{VCL}}$	0.1	8
$\mathbf{r_{BA}}$	1.2	8
$\mathbf{k_{a0}(L/s)}$	5.7×10^{-24}	This work
$\mathbf{k_{mov01}(1/s)}$	1×10^{-7}	4
$\mathbf{k_{mov02}(L/s)}$	8×10^{-10}	4
$\mathbf{k_{mov03}(1/s)}$	2×10^{-4}	4
$\mathbf{k_{d0}^{pol2}}$ **(mol/dm^2.s)**	5×10^{-15}	This work
$\mathbf{k_{n}(mol/s)}$	5×10^{-2}	4
$\mathbf{x_{c}}$ **(monomeric units)**	9×10^{5}	This work
$\mathbf{\bar{x}_{m}}$**(monomeric units)**	5×10^{3}	5

The radical concentration profile in the polymer particle was calculated via solving the following partial differential equation by orthogonal collocation on finite elements.[9]

$$\frac{\partial[R](t,r)}{\partial t} = \nabla^2 D_R[R](t,r) - k_t[R]^2(t,r) \qquad (S15)$$

$$\frac{\partial[R](t,0)}{\partial t} = 0;\ \ [R](t,rp) = [R]_s \qquad (S16)$$

$$\int_0^{r_p}[R]4\pi r^2 dr_p = \bar{n}\,/N_A \qquad (S17)$$

where D_R is the radical diffusion coefficient and k_t is the termination rate coefficient. $[R]_s$ is the radical concentration at the surface of the particle. The diffusion coefficient for radicals was reported to show a power-law variation with chain length[10]. In this work a constant kinetic chain length for the growing radical was assumed in the simulations (half of the degree of the polymerization of polymer 2, ($\bar{x}_m$) considering that termination reaction occurs by combination) and dependency parameter (β) was considered as adjustable:

$$D_R = \frac{D_M}{(\bar{x}_m/2)^{\beta}} \qquad (S18)$$

$$\log D_M = \log D^{\circ} - \frac{E}{2.303RT} - \frac{1}{2.303}\left[\frac{(1-w_2)\hat{V}_1^* + £w_2\hat{V}_2^*}{\frac{\hat{V}_f}{\gamma}}\right] \qquad (S19)$$

$$\frac{\hat{V}_f}{\gamma} = (1-w_2)\left(\frac{K_{11}}{\gamma}\right)(K_{21} + T - Tg_1) + w_2\left(\frac{K_{12}}{\gamma}\right)[K_{22} + a(T - Tg_p)] \qquad (S20)$$

where D° and E are the pre-exponential factor and activation energy of the monomer diffusion coefficient, respectively. a is the ratio between the coefficients of thermal expansion of the polymer below and above Tg of polymer. $\frac{K_{11}}{\gamma}$, $\frac{K_{12}}{\gamma}$,K_{21}, and K_{22} are free volume parameters. Tg_1 and Tg_p are monomer and polymer glass transition temperatures, respectively. T is the reaction temperature. $\hat{V}_1^*$ and $\hat{V}_2^*$ are specific volumes of monomer and polymer, respectively. w_2 is the weight fraction of polymer. £ is the size parameter[11] and $\frac{\hat{V}_f}{\gamma}$ is the solution free volume. The values of the parameters used are given in Table S3.

Figure S4 shows a representative radical concentration profile in the particle of mLNGs-1 with $[M](t,r)$=0.208 mol/L (corresponds to the $\phi_{Pol} = 0.971$) and Tg_{seed}= 195°C at $T_{reaction}$= 70°C. It can be shown that a sharp radical profile was generated, with the radical concentration decreasing rapidly towards the interior of the particle.

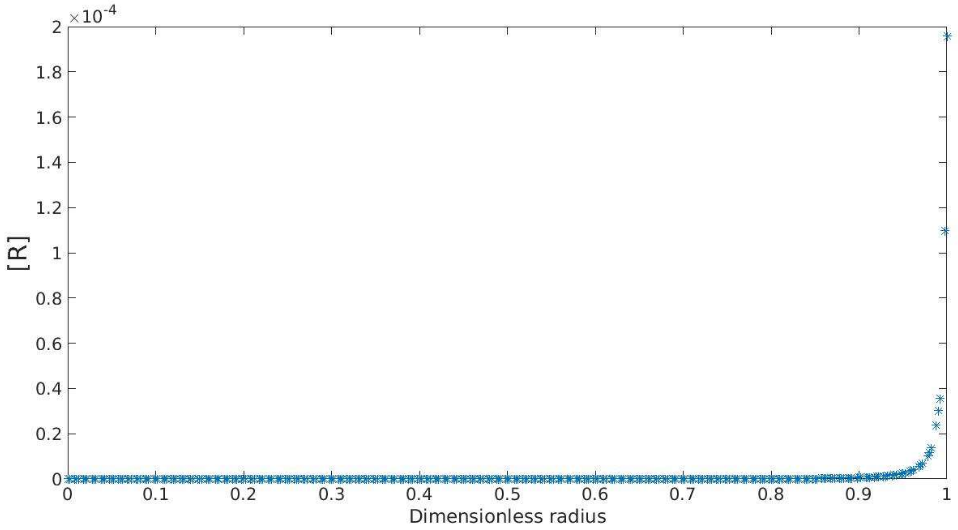

Figure S4. Radical concentration profile snapshot at t=70min in the particle (mol/L) with $D_R = 9 \times 10^{-17}$m2/s. ($[M](t,r)$= 0.208 mol/L (corresponds to the $\phi_{Pol} = 0.971$) and Tgseed= 195°C at Treaction= 70°C) PDE was solved using 100 elements and 4 collocation points at each element.

Table S3. Parameters for monomer and radical diffusion coefficient calculations (The parameters are for diffusion of MMA monomer in PMMA)

Parameter	**value**	**Reference**
D° (cm^2/s)	1.61×10^{-3}	11
E (cal/mol)	778	11
£	0.6	11
$\boldsymbol{\hat{V}_1^*}$ **(cm^3/g)**	0.87	11
$\boldsymbol{\hat{V}_2^*}$ **(cm^3/g)**	0.757	11
$\boldsymbol{\frac{K_{11}}{\gamma}}$ **(cm^3/g.K)**	0.815×10^{-3}	11
$\boldsymbol{K_{21}}$ **(K)**	143	11
$\boldsymbol{\frac{K_{12}}{\gamma}}$ **(cm^3/g.K)**	0.477×10^{-3}	11
$\boldsymbol{K_{22}}$ **(K)**	52.38	11
$\boldsymbol{a}$	0.44	11
$\boldsymbol{\beta}$	0.645	4

OVA release modelling

OVA release mechanism was evaluated though the power law model of Korsmeyer – Peppas (equation S21).[12]

$$\frac{M_t}{M_\infty} = kt^n \qquad \text{(S21)}$$

where $\frac{M_t}{M_\infty}$ represent the mass fraction of drug released at the time interval t, k is rate constant of drug release, and n is diffusion exponent.

The values of n fitted with results of Figure 12, together with the resulting correlation coefficients (R^2) can be found in **Table S4**.

Table S4. Diffusion exponent n obtained from data fit of OVA release of Figure 12 though Korsmeyer – Peppas model.

	n	R^2
mLNGs-1	0.44	0.945
mLNGs-2	0.49	0.982

REFERENCES

1 A. Imaz, J. I. Miranda, J. Ramos and J. Forcada, *Eur. Polym. J.*, 2008, **44**, 4002–4011.

2 A. Imaz and J. Forcada, *J. Polym. Sci. Part A Polym. Chem.*, 2008, **46**, 2510–2524.

3 N. A. Cortez-Lemus and A. Licea-Claverie, *Prog. Polym. Sci.*, 2016, **53**, 1–51.

4 N. Rajabalinia, University of Basque Country(UPV/EHU), 2019.

5 S. Hamzehlou, J. R. Leiza and J. M. Asua, *Chem. Eng. J.*, 2016, **304**, 655–666.

6 J. M. Asua, S. Beuermann, M. Buback, P. Castignolles, B. Charleux, R. G. Gilbert, R. A. Hutchinson, J. R. Leiza, A. N. Nikitin, J.-P. Vairon and A. M. van Herk, *Macromol. Chem. Phys.*, 2004, **205**, 2151–2160.

7 L. C. Kröger, W. A. Kopp and K. Leonhard, *J. Phys. Chem. B*, 2017, **121**, 2887–2895.

8 S. Verbrugghe, K. Bernaerts and F. E. Du Prez, *Macromol. Chem. Phys.*, 2003, **204**, 1217–1225.

9 B. A. Finlayson, L. T. Biegler and I. E. Grossmann, *Mathematics in Chemical Engineering*, Wiley-VCH Verlag GmbH & Co. KGaA, 2006.

10 G. B. Smith, G. T. Russell and J. P. A. Heuts, *Macromol. Theory Simulations*, 2003, **12**, 299–314.

11 A. Faldi, M. Tirrell, T. P. Lodge and E. Von Meerwall, *Macromolecules*, 1994, **27**, 4184–4192.

12 R. W. Korsmeyer, R. Gurny, E. Doelker, P. Buri and N. A. Peppas, *Int. J. Pharm.*, 1983, **15**, 25–35.